Functional Polymers for Electronics, Optics, and Renewable Packaging

Stingelin Lab @ Georgia Tech

Our current research interests encompass the broad field of functional materials for organic electronics; multifunctional inorganic/organic hybrids for smart, advanced optical systems; mixed conductors for bioelectronics; and materials for sustainable technologies. Establishing interrelationships between performance, processing, and materials' structure are thereby a central topic. Our group's multi-disciplinary efforts in the Materials Science field have been exploited to build collaborations across departments and faculties at Georgia Tech, on national level, and internationally.

Check out our lab's publications, scan this QR code:
Email: natalie.stingelin@mse.gatech.edu
Web: stingelin-lab.gatech.edu/
@StingelinGroup

Materials for sustainable and renewable technologies

Transparent IR mirrors and thermal switches for heat management (with Yee Lab)

IR mirrors made of hybrid materials can reflect the sun's radiation and potentially cool a building. Thermal switches can dynamically control the amount of heat flow.

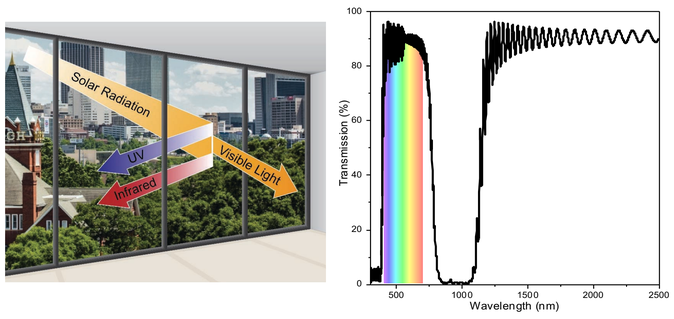

Figure 1: Window coatings based on Distributed Bragg Reflectors (DBR's) with stopband tunable to infrared, while transmitting visible wavelengths.

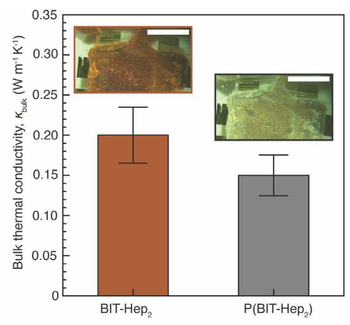

Figure 2: Reversible polymerization results in a change in thermal conductivity

Biomaterials for sustainable packaging (with Meredith and Kyriaki Labs)

Sustainable packaging is enabled by blending and crosslinking renewably-derived polymers and nanomaterials to improve gas barrier performance and recyclability.

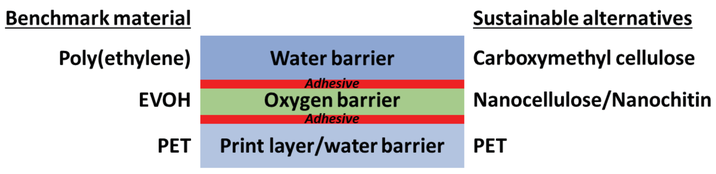

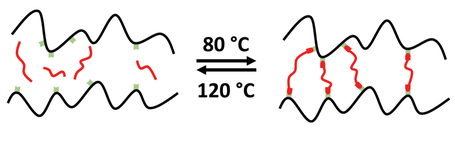

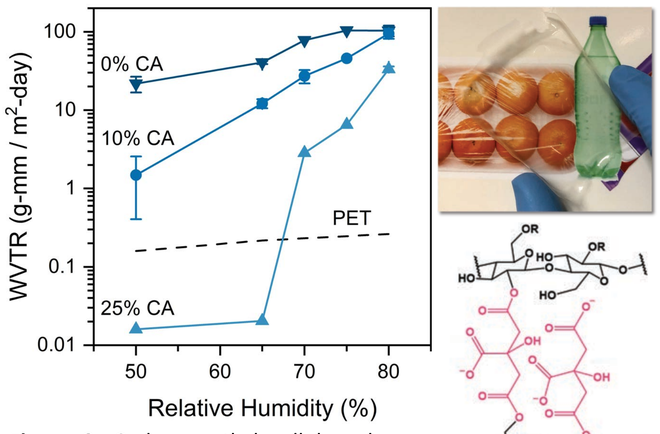

Figure 3: Carboxymethyl cellulose has a lower water vapor transmission rate than PET when crosslinked by citric acid (CA).

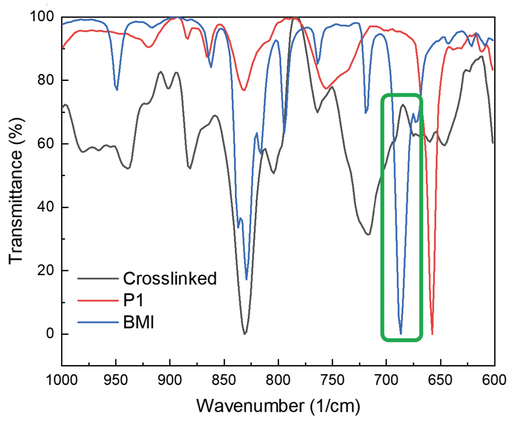

Figure 4: FTIR spectra showing thermo-reversible crosslinks for designing releasable adhesive layers to make more recyclable multilayer plastics.

Structure-property relationship of semiconductors and blends

Organic semiconductor devices (e.g., OPVs, OFETs, thermoelectrics) rely on a unique property set derived from specific material and its combinations. However, structure-property relationship of such semiconductor materials and their blends, e.g., with respect to transport properties, are not well understood. Here, we focus on different polymers and their blends in order to gain deeper insights into them.

Processing induced liquid-crystalline phases

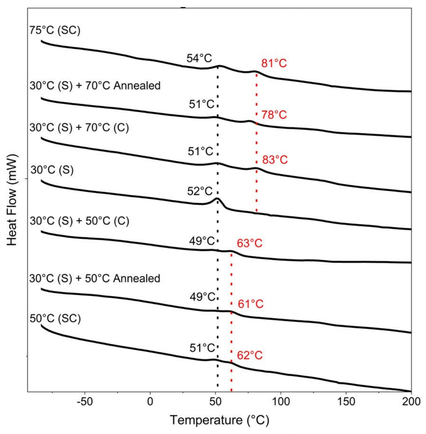

Figure 5: Processing PBTTT under pressure and sufficiently high temperatures induces increased order of liquid crystalline phase indicated by a unique enthalpic recovery at 61 °C and secondary endothermic peaks at 82°C.

Semiconducting/polar polymer blends

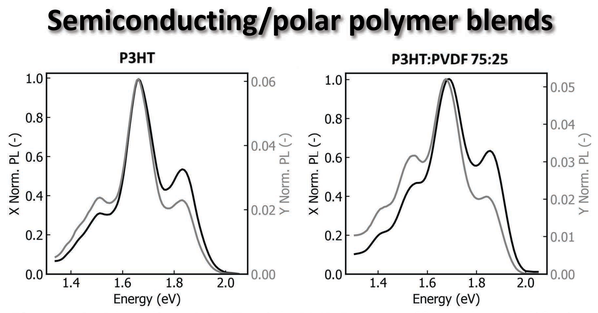

Figure 6: Blending P3HT with PVDF may affect the PL lifetime, due to the high dielectric constant of PVDF. We observe a dramatic change in the lineshape of the prompt (X) and delayed (Y) PL, indicating that delayed PL stems from regions of the film with different local ordering.

Liquid-crystalline and birefringent materials

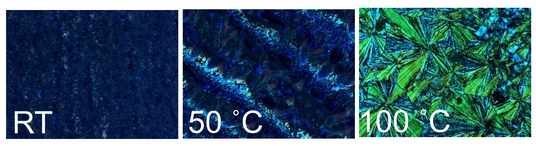

Figure 7: ITIC is a non-fullerene acceptor that undergoes phase transitions when blended and subject to temperature.

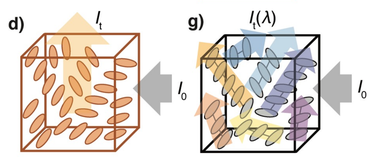

Figure 8: This diagram illustrates a monomer that is not birefringent (left), and a polymer with the same repeat unit that is birefringent due to the orientation of the polymer chains (right).

Inorganic-organic hybrid materials

Mixed conduction materials exhibit simultaneous electronic and ionic conductivity, enabling direct interfacing between electronics and electrochemical systems. Potential applications for mixed conduction include batteries, synthetic neural and cardiomyocyte tissue scaffolds, and biosensors, amongst others.

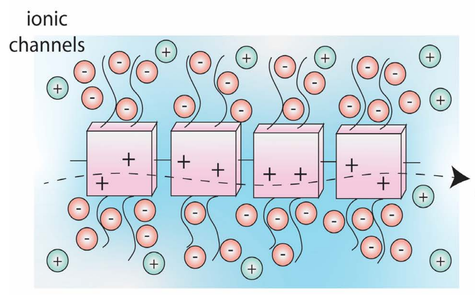

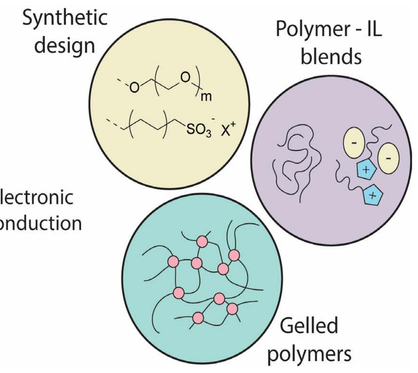

Reversible swelling of semiconducting copolymer with hydrophilic sidechains (with Reynolds Lab)

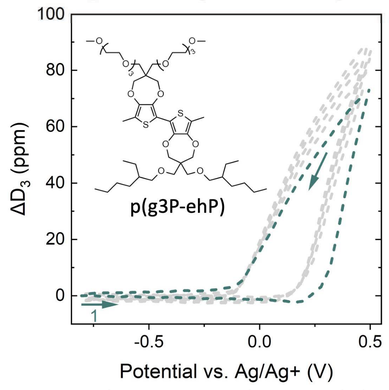

Figure 9: Neutral ProDOT copolymer with 'amphiphilic' aliphatic and oligoether sidechains swells and deswells reversibly, as shown by electrochemical quartz crystal microbalance with dissipation monitoring

Mechanical properties of hybrid gels

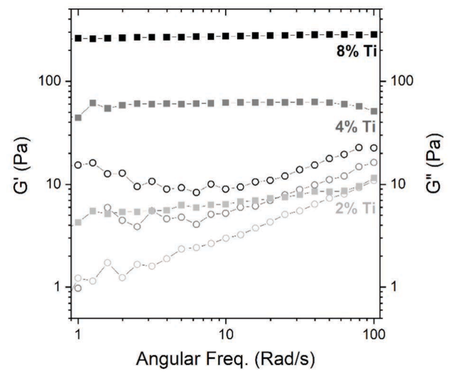

Figure 10: Increasing titanium oxide hydrate content in inorganic:organic hybrids with poly(vinyl alcohol) results in higher storage and loss moduli, associated with a higher density of crosslinks.

Fully solution-processable microcavities (with Silva Lab)

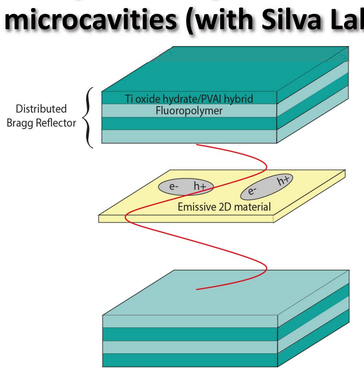

Figure 11: Structure of a solution-processed microcavity enabled by multilayers of alternating refractive index and thickness.

Capacitive sensors for UV detection

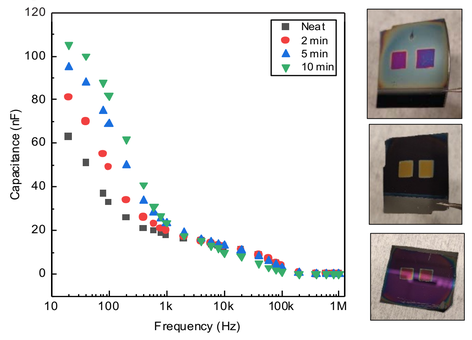

Figure 12: Flexible capacitive UV sensors based on polyvinyl alcohol is enabled by manipulating the hydrated titanium oxide concentrations to change the capacitance when exposed to UV doses.

Local ordering of semiconducting polymers

Local ordering affects electrostatic, Coulombic, and general photophysical processes in semiconducting polymers. Thus, understanding the impact of local ordering in these materials is crucial to optimizing them.

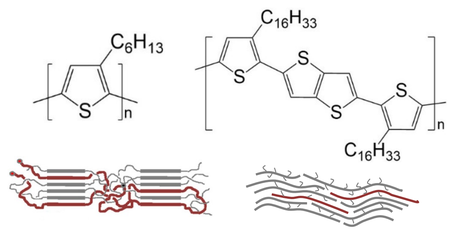

Figure 13: Chemical structure and schematics of P3HT (left) and PBTTT (right).

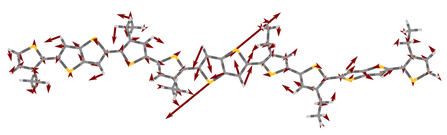

Figure 14: Vector graph of one vibrational pattern of PBTTT oligomer.

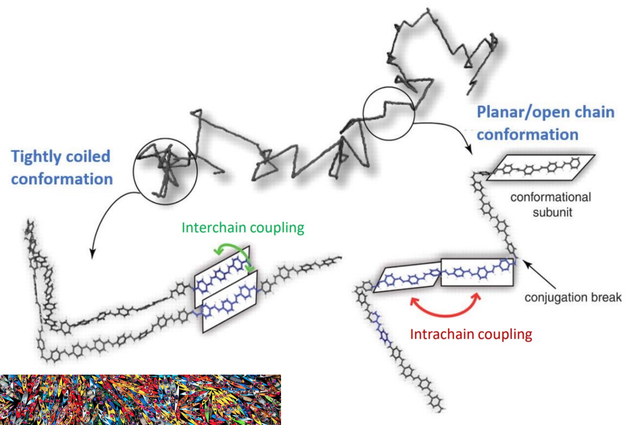

Figure 15: Kayaks can be thought of as rigid repeat units. Here, we see local order due to the rigid "backbone" of the kayak (*National Geographics*).

Manipulating and Characterizing Local Order of Semiconducting Polymers

Stingelin Lab at Georgia Tech

SPECS Center for Soft PhotoElectroChemical Systems

Unraveling differences in disorder of flexible-chain and hairy-rod polymers

P3HT
Structurally heterogeneous

PBTTT
Structurally homogeneous

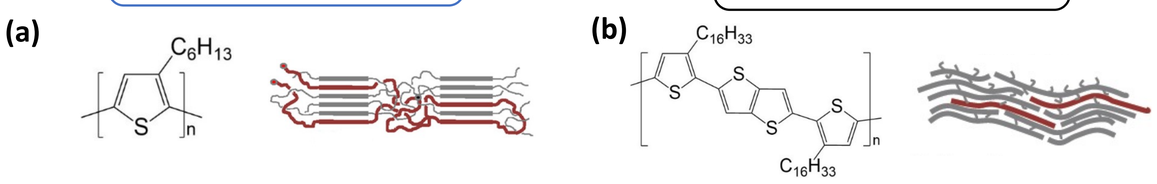

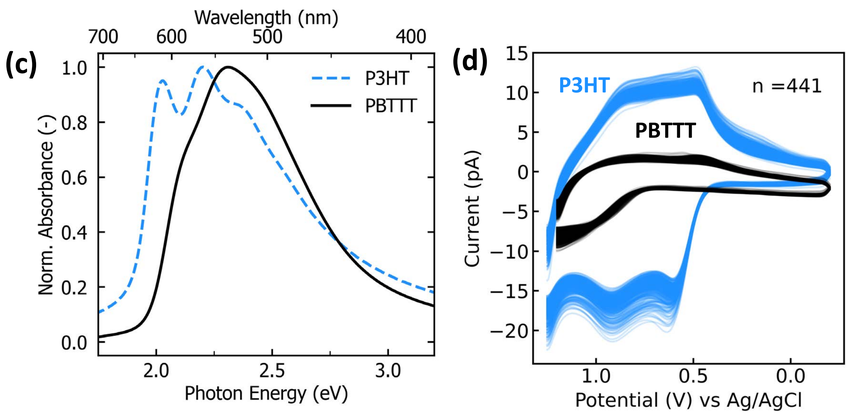

Figure 1: Optoelectronic and electrochemical indications of disorder. Chemical structure and microstructure of (a) P3HT and (b) PBTTT. (c) Linear absorption linewidths of P3HT and PBTTT are similarly broadened. (b) Nanoscale CVs of P3HT are highly spatially variable, while PBTTT features a much tighter current distribution.

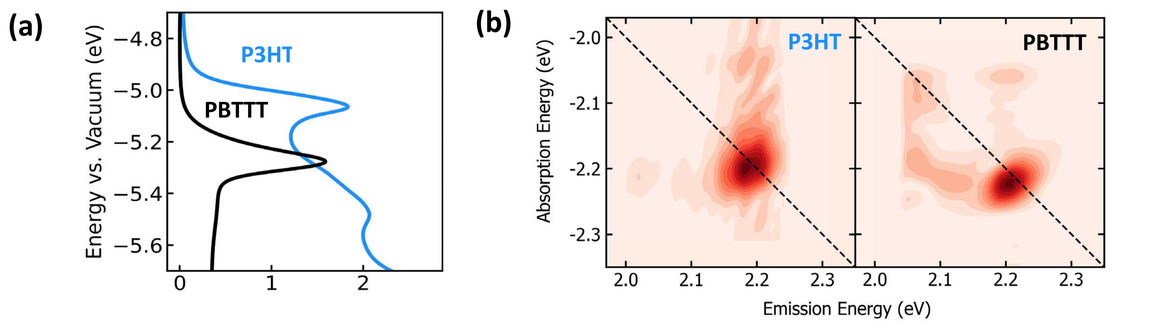

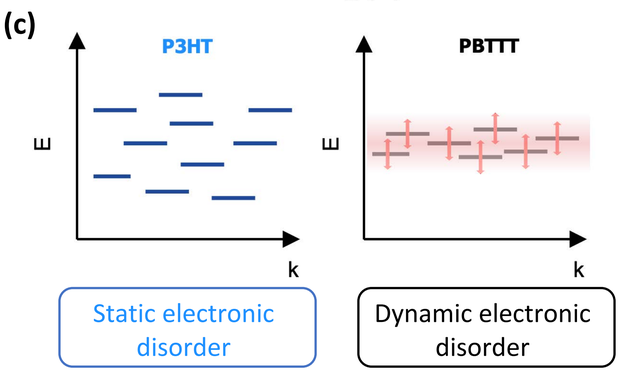

Figure 2: Correlating structural and electronic disorder. (a) Macroscale electrochemistry identifies a broader density of states (DOS) distribution for P3HT than for PBTTT. (b) 2D electronic spectroscopy separates contributions from static vs. dynamic electronic disorder. (c) Proposed energy level distribution diagrams for flexible-chain and hairy-rod polymers.

Ratcliff and Silva Group Collaboration

Disentangling the complexities of polymer:polymer phase morphology

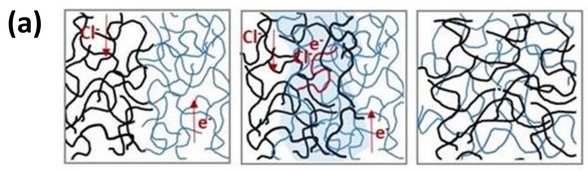

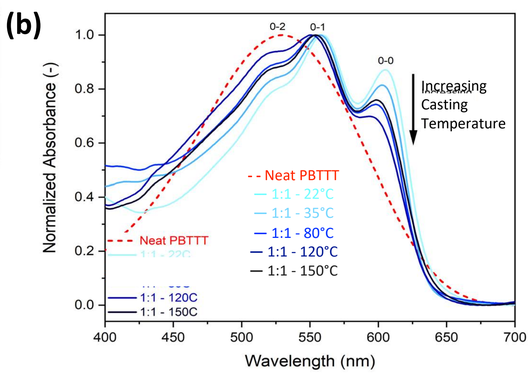

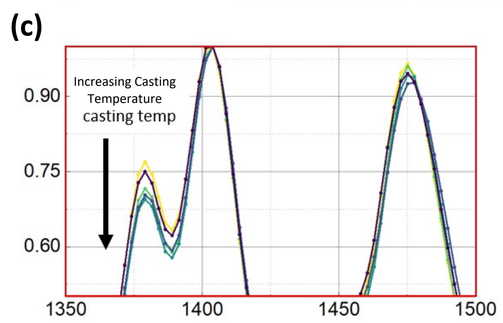

Figure 3: Manipulating phase morphology in polymer:fullerene blends. (a) Schematic of phase separated vs. intermixed polymer in electrolyte. (b) UV-VIS absorbance spectra of neat and binary PBTTT:PCBM. (c) Raman spectra of binary PBTTT:PCBM showing impact of intercalation vs phase separation.

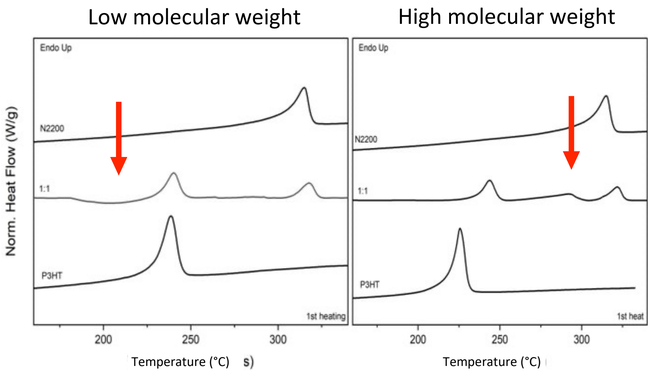

Polymer:fullerene blends provide an excellent model system for studying more complex D:A blends

Figure 4: Controlling intermixing in P3HT:N2200 blends via chain entanglements. DSC of (a) a phase separated blend of low M_w (60:20 kg/mol) P3HT:N2200 and (b) an intermixed, high M_w (130:20 kg/mol) P3HT:N2200 blend.

Lian Group Collaboration

Fast-scanning calorimetry to investigate phase behavior of hairy-rod polymers

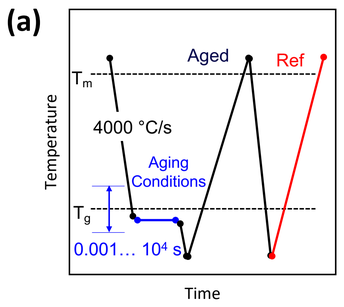

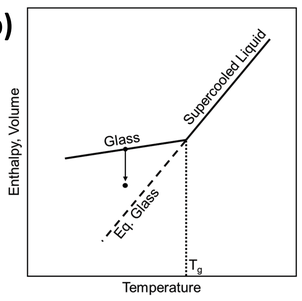

Figure 5: Fast differential scanning calorimetry of a hairy-rod polymer to estimate the glass transition temperature. (a) Overview of the physical aging experiment. (b) Representation of structural recovery during aging. (c) Conventional DSC of N2200. (d) Fast DSC of N2200.

N2200

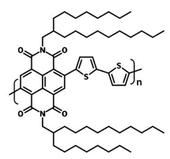

FDSC identifies thermal transitions not seen in conventional DSC

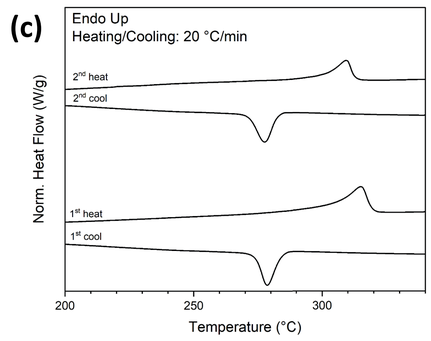

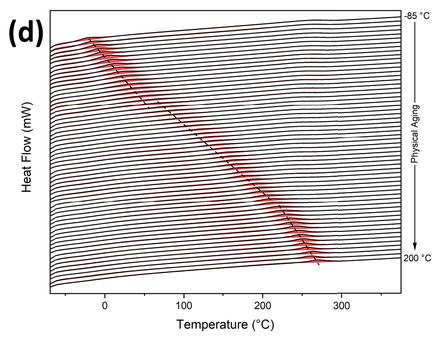

Risko/Brédas Group Collaboration

Local order in hairy-rod polymer:electrolyte interphases

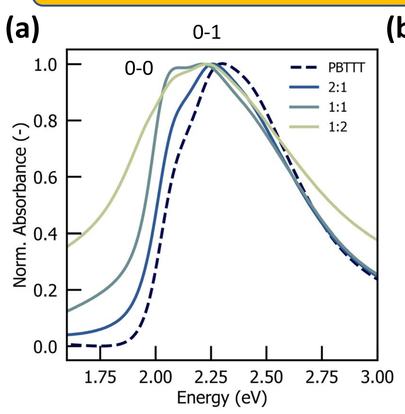

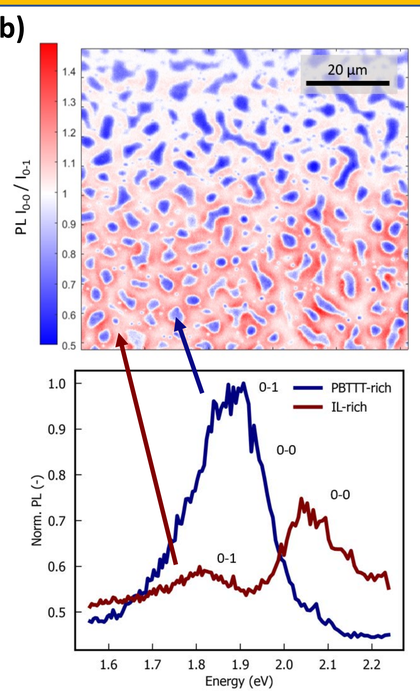

PBTTT

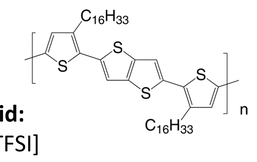

Ionic Liquid:
[C12mim][TFSI]

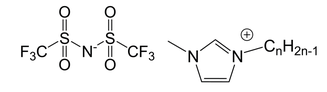

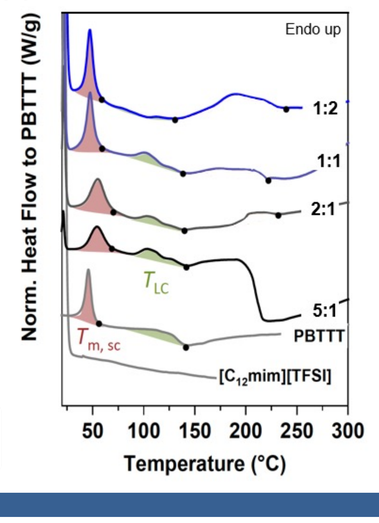

Figure 6: Manipulating H/J aggregation by blending a hairy-rod polymer with an ionic liquid. (a) Linear absorbance of the PBTTT:IL blends. (b) Hyperspectral PL of the 1:2 blend highlights differences in aggregation between IL-rich and PBTTT-rich domains. (c) DSC suggests the presence of two LC phases that vary with blend composition.

Electrolyte-rich domains are not phase-pure and more J-like

Ratcliff Group Collaboration

Separating structural and dielectric effects on exciton recombination

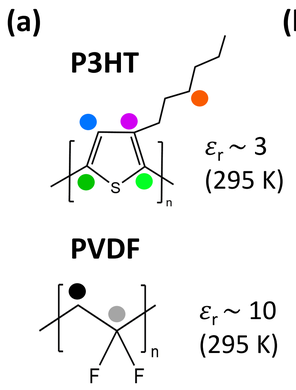

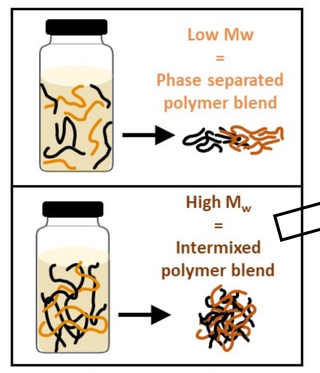

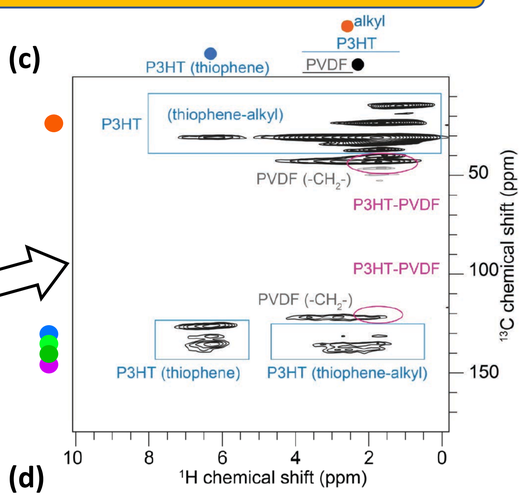

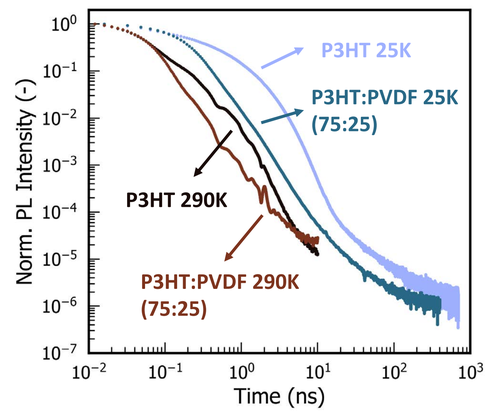

Figure 7: Photophysics of conjugated polymers in high dielectric environments. (a) Structure of P3HT and PVDF. (b) Schematic of morphology control via chain entanglements. (c) Solid-state NMR suggests nanoscale mixing of high M_w P3HT:PVDF blends. (d) Time-resolved photoluminescence of P3HT and P3HT:PVDF to probe exciton recombination processes.

Vitrified microstructure leads to faster exciton recombination, despite increased dielectric environment.

NREL and Reddy Group Collaboration